

NORMAL SIMILARITY NETWORK FOR GENERATIVE MODELLING

Jay Nandy, Wynne Hsu, Mong Li Lee

School of Computing, National University of Singapore

ABSTRACT

Gaussian distributions are commonly used as a key building block in many generative models. However, their applicability has not been well explored in deep networks. In this paper, we propose a novel deep generative model named as Normal Similarity Network (NSN) where the layers are constructed with Gaussian-style filters. NSN is trained with a layer-wise non-parametric density estimation algorithm that iteratively down-samples the training images and captures the density of the down-sampled training images in the final layer. Additionally, we propose NSN-Gen for generating new samples from noise vectors by iteratively reconstructing feature maps in the hidden layers of NSN. Our experiments suggest encouraging results of the proposed model for a wide range of computer vision applications including image generation, styling and reconstruction from occluded images.

Index Terms— Deep Generative Model, Image Generation, Non-parametric Training

1. INTRODUCTION

Unsupervised learning, where no labels are provided during training, remains one of the core challenges in machine learning. One branch of unsupervised learning that is popular in image processing/computer vision is the generative models that aim to obtain a representation of the density function, p_{model} to describe the density of a given data domain, p_{data} . Auto-regressive models such as Fully Visible Belief Nets [1], PixelRNN [2], explicitly model the joint distribution of pixels as a product of conditional distributions and optimize the likelihood of training data. However, due to higher dimension and the structured formation of images, modelling the long-range pixel correlation becomes challenging for these explicit tractable density models. Instead of designing an explicit tractable model, Variational Autoencoder (VAE) [3, 4]) approximates the likelihood by maximizing a lower bound. This is achieved with an encoder-decoder neural network architecture. The encoder’s output fits a prior distribution by minimizing the KL-divergence. The decoder then transforms encoder’s output to reconstruct the images. In practice, they often achieve higher likelihood values, however, fails to generate sharp images [5].

Generative Adversarial Networks (GANs) offer an alter-

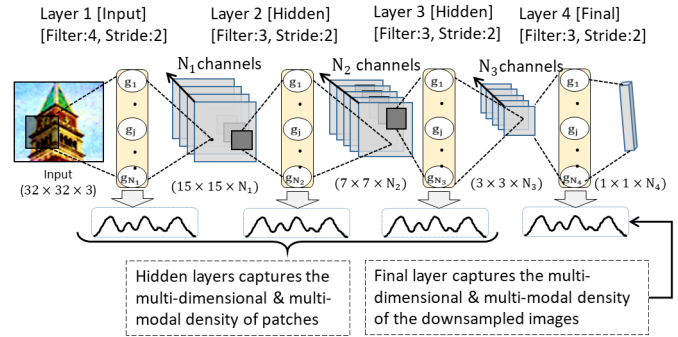


Fig. 1: Schematic diagram of a 4-layered NSN. Each layer of NSN captures the density of patches via likelihood maximization criterion and downsamples the images. After down-sampling the training images, the final layer captures the density of them in a transformed domain.

native solution that draw samples from p_{data} to learn an implicit density function through a minimax formulation [6, 7, 8, 9, 10]. However, GANs often suffer from training instability [11]. Although recent progresses for GANs aim to address this issue by replacing the Jensen-Shannon divergence (JSD) [12, 10, 9], the new formulations generally can not address the mode collapsing problem where the generator can only accommodate a few modes in the training domain [7]. Tricks such as feature matching, mini-batch discrimination [13] or by unrolling multiple steps during the gradient update in training [14], handle this issue to some extent.

In this paper, we develop a deep generative model that shares the properties of both explicit density models such as PixelRNN, VAE as well as implicit density models such as GAN. We propose a Normal Similarity Network (NSN) with multiple hidden layers where every layer is constructed with learnable Gaussian-style filters. Figure 1 presents a schematic diagram of NSN. The proposed model downsamples the images and explicitly captures the density in a transformed domain via likelihood maximization. Further, we propose a sampling approach, NSN-Gen, to generate new images from NSN. NSN-Gen takes a noise vector as input at the final layer and performs a backward pass to generate the pixels in parallel. In our experiments, we demonstrate the applicability of NSN to a wide range of tasks including image generation, image styling and reconstruction from occluded images.

	Autoregressive (eg. PixelRNN)	Variational (VAEs)	Adversarial (GANs)	NSN (Ours)
Lower model complexity?	✓	✗	✗	✓
Non-parametric modelling?	✗	✗	✗	✓
Stable training?	✓	✓	✗	✓
Parallel pixel generation?	✗	✓	✓	✓
Sampling from hidden layers?	✗	✗	✗	✓

Table 1: Table to compare the characteristics of the proposed NSN with the existing deep generative models.

Table 1 provides a comparison of the characteristics of our proposed NSN with existing deep generative models. In terms of model complexity, NSN requires to maintain only a single network constructed with Gaussian-like filters, whereas GANs or VAEs require two or more neural networks. Furthermore, PixelRNN, VAE and GAN all are constructed as a parametric network. In contrast, NSNs support non-parametric training that can automatically detect the required number of filters at each layer of the network. The NSNs are trained with a variant of the Expectation Maximization (EM) algorithm which has been shown to have a direct and stable density estimation process [15]. In addition, our generation algorithm, NSN-Gen, can be applied at any hidden layer to visualize the image patches generated at that layer, thus enabling fine tuning of the network.

2. NORMAL SIMILARITY NETWORK

The NSN architecture is inspired from CNN-based models where the layers are constructed with learnable Gaussian-style filters [16, 17]. The inputs are image patches obtained by sliding a window over an image with some stride step. We represent each image patch as a multi-dimensional array $\mathbf{x}_i, i = 1, 2, \dots$. At each layer, we compute the similarity scores of the image patches to the filters, and apply a sigmoid activation function to ensure that the outcomes fall in the range $[0, 1]$. These sigmoid activation maps of similarity scores are the outputs of each layer. Note that, the output of the final layer is one-dimensional feature maps (refer to Figure 1).

We use a variant of Expectation-Maximization (EM) algorithm at each layer to learn the filters by maximizing the log-likelihood of the image patches [15]. Our non-parametric EM is a hard clustering model that automatically determines the required number of filters at each layer. We start with one filter $g_1(\boldsymbol{\mu}_1, \sigma_1)$ where $\boldsymbol{\mu}_1$ and σ_1 are randomly initialized, and iteratively create new filters as follows. Each iteration consists of an E-Step and an M-Step.

In the E-Step, we compute the similarity of each image patch \mathbf{x}_i to the filter $g_j(\boldsymbol{\mu}_j, \sigma_j), 1 \leq j \leq N$, where N is the

number of existing filters. The similarity score is given as:

$$Sim(\mathbf{x}_i, g_j(\boldsymbol{\mu}_j, \sigma_j)) = \log \left(\frac{1}{\sqrt{2\pi}\sigma_j} \exp -\frac{\|\mathbf{x}_i - \boldsymbol{\mu}_j\|^2}{2\sigma_j^2} \right), \quad (1)$$

where $\|\cdot\|$ is the L_2 -norm. The filter mean, $\boldsymbol{\mu}_j$ is a tensor of same dimension as \mathbf{x}_i and $\sigma_j \in \mathbb{R}$ is a scalar value. We assign the image patch to the filter with the highest similarity score. If this score is lower than some pre-defined threshold α , we assign the patch to a new filter.

In the M-step, we update the parameters of each filter g_j :

$$\boldsymbol{\mu}_j^{new} = \frac{1}{|S|} \sum_{\mathbf{x}_i \in S} \mathbf{x}_i, \quad (2)$$

$$\sigma_j^{new} = \sqrt{\frac{1}{|S|} \sum_{\mathbf{x}_i \in S} \|\mathbf{x}_i - \boldsymbol{\mu}_j^{new}\|^2}, \quad (3)$$

where S be the set of patches assigned to filter g_j . The algorithm terminates when converged or the number of iterations exceeds the maximum limit.

3. IMAGE GENERATION FROM NSN

The final layer of NSN captures the density of downsampled training images in an one-dimensional vector space. Our proposed image generation algorithm, NSN-Gen takes a random vector from that vector space as input and generates a new image through a backward pass.

Let us assume, there is L layers in NSN and the number of filters at layer k is denoted as N_k . Let \mathbf{F}_k be the feature maps at layer k . We start the process from layer L with \mathbf{F}_L as a random $1 \times 1 \times N_L$ dimensional noise sampled from a normal distribution $\mathcal{N}(\mathbf{0}, \mathbf{1})$. NSN-Gen iteratively reconstructs the feature maps while progressing towards the input layer to generate an image (refer to Figure 2).

After reconstructing $\mathbf{F}_k, \mathbf{F}_{k-1}$ is produced by generating its patches as a weighted combination of the samples drawn from the N_k filters of layer k . The weights of the samples corresponding to the $(r, c)^{th}$ patch is obtained by processing the vector \mathbf{v} , at $(r, c)^{th}$ entry of \mathbf{F}_k . We increase the dynamic range of \mathbf{v} by an element-wise exponential function, $\tilde{\mathbf{v}} \propto \exp(\delta_1 \mathbf{v})$ followed by a normalization, where δ_1 is a hyper-parameter. We construct the weight vector \mathbf{w} by sampling n ($\ll N_k$) filter indices of layer k with replacement policy and normalizing the sample counts:

$$\mathbf{w} \sim Multinomial(n, \tilde{\mathbf{v}}), \quad (4)$$

where $\tilde{\mathbf{v}}$ represents the probability distribution of the multinomial distribution. We store \mathbf{w} into the $(r, c)^{th}$ position of a weight map \mathbf{W}_{k-1} . Now, we draw samples $\mathbf{Y} = [\mathbf{y}_1, \dots, \mathbf{y}_{N_k}]$ from filters $g_j(\boldsymbol{\mu}_j, \sigma_j), 1 \leq j \leq N_k$:

$$\mathbf{y}_j = \boldsymbol{\mu}_j + \delta_2 \sigma_j \mathbf{M}, \quad (5)$$

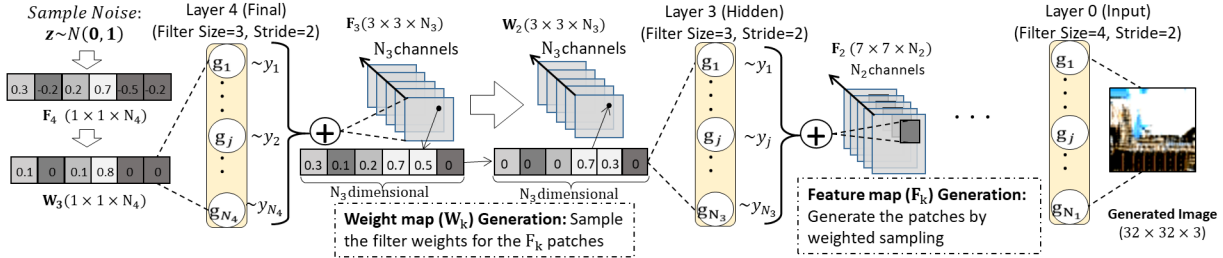


Fig. 2: Example of image generation process from a 4-layered NSN: Sample the final layer feature map, F_4 from $\mathcal{N}(\mathbf{0}, \mathbf{1})$. NSN-Gen then constructs the weight map W_3 , for the patches of F_3 . We then generate the patches by combining samples drawn from 4th layer filters. The process continues until we reach in the input layer to generate the image.

where $M \sim \mathcal{N}(\mathbf{0}, \mathbf{1})$ is a random matrix of the same dimension as μ_j . Finally, we generate the patch $(\delta_3 \mathbf{w}^T \mathbf{Y})$ as the weighted sum of these samples, where δ_2 and δ_3 are hyper-parameters. After obtaining the patches for all (r, c) positions, we stitch them together by averaging the overlapped regions to obtain F_{k-1} . Similarly, this method can be applied to draw samples from a hidden layer k . Starting with an $1 \times 1 \times N_k$ dimensional noise vector at layer k the same process is repeated till the input layer. As NSN-Gen can be applied at any hidden layer to reconstruct the upper layer feature maps, it allows us to applied to a wide range of computer vision problems as demonstrated in the next section.

4. EXPERIMENTS

We use four different datasets in our experiments: MNIST [18] and Fashion [19] contains 28×28 gray scale images of hand written digits and cloths. LFW [20] and Church [21] are RGB images of human faces and church buildings that are resized to 64×64 . For the LFW dataset, we preprocess the images with channel-wise ZCA transformation as this enables our network to generate sharper human face images. We train 3-layer NSNs for MNIST and Fashion and 5-layer NSNs for LFW and Church datasets. The required number of filters at each layer are automatically determined during training.

4.1. Comparative Study

We carry out a qualitative comparison of the samples generated by the proposed NSNs with state-of-the-art GAN models. We compute the inception score with 50,000 samples randomly generated by these models [13]. A higher Inception Score is achieved if a pre-trained inception convolutional network classifies the samples with higher certainty as well as identifies a diverse variety among them. Table 2 shows that the samples generated from NSN are comparable with the state-of-the-art models. Figure 3 shows the NSN-generated samples of MNIST and Fashion. Figure 4 presents the Church and LFW samples generated by DCGAN [8], WGAN [10], LSGAN [9] and our NSN for visual comparison.

	MNIST	Fashion	LFW	Church
Real Data	1.99 ± 0.01	4.25 ± 0.05	3.64 ± 0.28	2.70 ± 0.04
DCGAN [8]	2.27 ± 0.01	4.15 ± 0.04	2.67 ± 0.03	2.89 ± 0.02
WGAN [10]	2.02 ± 0.02	3.00 ± 0.03	2.94 ± 0.03	3.05 ± 0.02
LSGAN [9]	2.03 ± 0.01	4.45 ± 0.03	2.33 ± 0.02	3.44 ± 0.04
NSN (Ours)	2.44 ± 0.02	3.85 ± 0.04	3.04 ± 0.10	2.99 ± 0.02

Table 2: Inception score calculated on 50,000 images randomly sampled from GAN models and our proposed NSNs. Score for LFW(Real Data) is calculated for entire dataset of 13,233 images. Higher scores are better.



Fig. 3: Visualization of generated samples from NSN.

4.2. Effect of NSN-Gen hyper-parameters

We use the same values for the hyper-parameters (δ_1 , δ_2 and δ_3) across different layers for NSN-Gen. They are selected to maximize the inception score. We can control the characteristics of generated images by these hyper-parameters. Figure 5, shows the generated images as we vary one of them while keeping same values for the others. As we increase δ_1 , it increases the dynamic range of filter similarity scores. As a result, choosing the filter with maximum similarity score becomes more probable (Eq 4), resulting generation of uniform and sharper images. However, a very large value for δ_1 reduces the diversity among the generated patterns and thereby reduces the inception score. δ_2 influences the pixel randomness while δ_3 controls the contrast for the generated images.

4.3. Applications of NSNs

In this section, we show how NSN can be also used for image styling and reconstruction of occluded images. For these applications, we train NSNs with images preprocessed with channel-wise ZCA whitening. This preprocessing is useful to remove correlations which may exist among the neighbor-

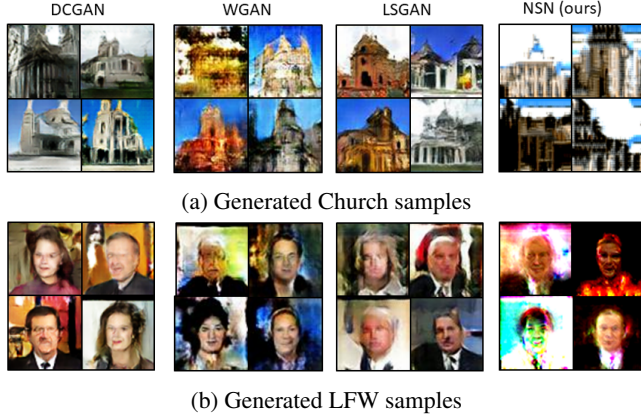


Fig. 4: Visualization of the best samples generated by different state-of-the-art GAN models and our proposed NSN.

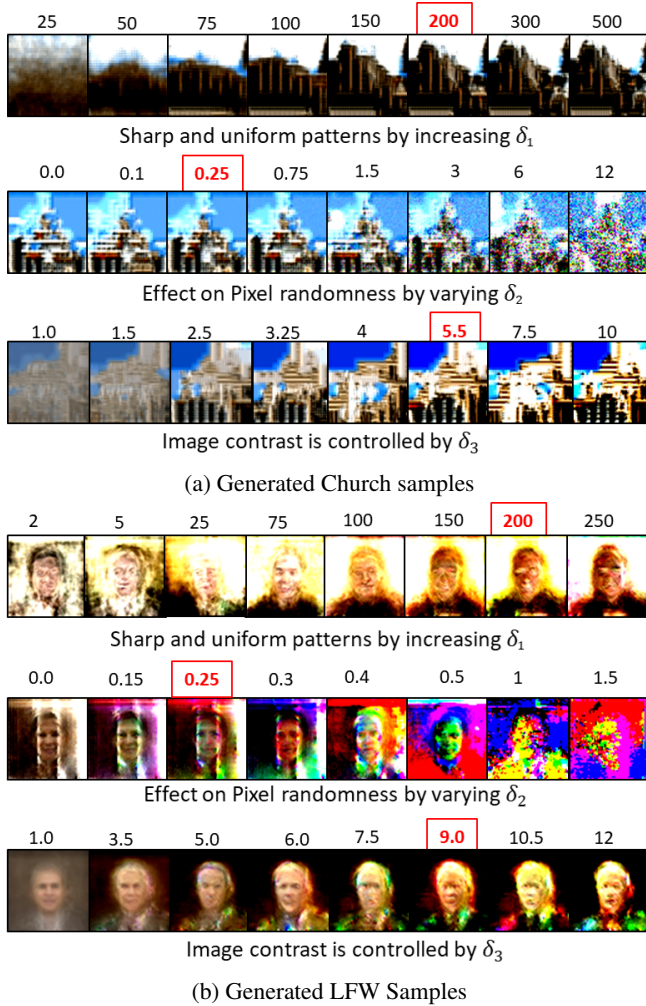


Fig. 5: Visualizing the effect of NSN-Gen hyper-parameters ($\delta_1, \delta_2, \delta_3$) on the generated images. Values in the red boxes presents the selected hyper-parameters for computing the inception scores. We vary one of the three hyper-parameters at each row to produce the images from the same noise vector.

hood pixels in natural images. This allows us to obtain evenly distributed filters over the input patches [22].

Image Styling. Image styling is an attractive and emerging field in computer vision with many successful industrial applications [23]. As we downsample an image into the NSN and reconstruct back from its first layer feature map, the network adds a fractal style in the image. Figure 6 shows that NSN-Gen is able to generate many different style images for the same input image due to its inherent sampling properties.

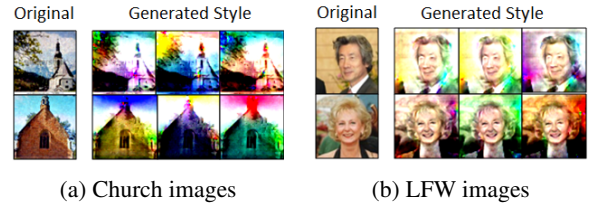


Fig. 6: Example of generated style images using NSNs.

Reconstruction of Ocluded Images. As the final layer of an NSN captures the density in a transformed training domain, the final layer feature maps of an occluded image should represent feature maps of a valid image. Here, we aim to reconstruct the occluded portion by conditioning on this final layer feature map. We start with this final layer feature map and apply NSN-Gen to reconstruct the occluded portion in its first layer feature map. The image is then reconstructed from this modified first-layer feature map that appropriately fills the occluded part as shown in Figure 7. Note that, in many cases, this procedure loses the color information due to the ZCA preprocessing and reconstruction errors introduced by NSN-Gen. However, we can add colors and style on these generated images by adjusting the NSN-Gen hyper-parameters.

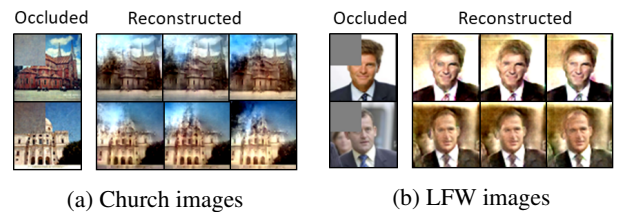


Fig. 7: Example of occluded image reconstruction by NSN.

5. CONCLUSION

Generative modelling with NSN presents an encouraging direction for unsupervised image modelling that aims to learn the density function of the final layer activation maps of the training images by maximizing the likelihood. The proposed NSN-Gen presents a technique to generate images from a noise vector by reconstructing activation maps at each layers. Experiments suggest that once the model is trained, it can be adopted for various computer vision applications.

References

- [1] Brendan J. Frey, Geoffrey E. Hinton, and Peter Dayan, “Does the wake-sleep algorithm produce good density estimators?,” in *International Conference on Neural Information Processing Systems*, 1995, pp. 661–667.
- [2] Aäron Van Den Oord, Nal Kalchbrenner, and Koray Kavukcuoglu, “Pixel recurrent neural networks,” in *International Conference on Machine Learning*. 2016, pp. 1747–1756, JMLR.org.
- [3] Diederik P. Kingma and Max Welling, “Auto-encoding variational bayes,” in *International Conference on Learning Representations (ICLR)*, Apr. 2014.
- [4] Danilo Jimenez Rezende, Shakir Mohamed, and Daan Wierstra, “Stochastic backpropagation and approximate inference in deep generative models,” in *International Conference on Machine Learning (ICML)*, 2014, vol. 32, pp. 1278–1286.
- [5] Ian Goodfellow, Yoshua Bengio, and Aaron Courville, *Deep Learning*, MIT Press, 2016.
- [6] Ian Goodfellow, Jean Pouget-Abadie, Mehdi Mirza, Bing Xu, David Warde-Farley, Sherjil Ozair, Aaron Courville, and Yoshua Bengio, “Generative adversarial nets,” in *Advances in Neural Information Processing Systems (NIPS)*, 2014, pp. 2672–2680.
- [7] Ian J. Goodfellow, “NIPS 2016 tutorial: Generative adversarial networks,” *CoRR*, 2017.
- [8] Alec Radford, Luke Metz, and Soumith Chintala, “Unsupervised representation learning with deep convolutional generative adversarial networks,” in *International Conference on Learning Representations (ICLR)*, 2016.
- [9] Guo-Jun Qi, “Loss-sensitive generative adversarial networks on lipschitz densities,” *CoRR*, vol. abs/1701.06264, 2017.
- [10] Martin Arjovsky, Soumith Chintala, and Léon Bottou, “Wasserstein generative adversarial networks,” in *International Conference on Machine Learning (ICML)*, 2017, pp. 214–223.
- [11] Martin Arjovsky and Léon Bottou, “Towards principled methods for training generative adversarial networks,” in *International Conference on Learning Representations (ICLR)*, 2017.
- [12] Sebastian Nowozin, Botond Cseke, and Ryota Tomioka, “f-gan: Training generative neural samplers using variational divergence minimization,” in *Advances in Neural Information Processing Systems (NIPS)*, 2016, pp. 271–279.
- [13] Tim Salimans, Ian J. Goodfellow, Wojciech Zaremba, Vicki Cheung, Alec Radford, and Xi Chen, “Improved techniques for training gans,” in *Advances in Neural Information Processing Systems (NIPS)*, 2016.
- [14] Luke Metz, Ben Poole, David Pfau, and Jascha Sohl-Dickstein, “Unrolled generative adversarial networks,” in *International Conference on Learning Representations (ICLR)*, 2017.
- [15] Christopher M. Bishop, *Pattern Recognition and Machine Learning*, Springer, 2006.
- [16] S. Lawrence, C.L. Giles, Ah Chung Tsoi, and A.D. Back, “Face recognition: a convolutional neural-network approach,” *Neural Networks, IEEE Transactions on*, vol. 8, no. 1, pp. 98–113, Jan. 1997.
- [17] Alex Krizhevsky, Ilya Sutskever, and Geoffrey E. Hinton, “Imagenet classification with deep convolutional neural networks,” in *Advances in Neural Information Processing Systems (NIPS)*, 2012, pp. 1097–1105.
- [18] Yann LeCun, “The mnist database of handwritten digits,” <http://yann.lecun.com/exdb/mnist/>, 1998.
- [19] Han Xiao, Kashif Rasul, and Roland Vollgraf, “Fashion-mnist: a novel image dataset for benchmarking machine learning algorithms,” 2017.
- [20] Gary B. Huang, Manu Ramesh, Tamara Berg, and Erik Learned-Miller, “Labeled faces in the wild: A database for studying face recognition in unconstrained environments,” Tech. Rep. 07-49, University of Massachusetts, Amherst, October 2007.
- [21] Fisher Yu, Yinda Zhang, Shuran Song, Ari Seff, and Jianxiong Xiao, “LSUN: construction of a large-scale image dataset using deep learning with humans in the loop,” *CoRR*, vol. abs/1506.03365, 2015.
- [22] Adam Coates and Andrew Y. Ng, “Learning feature representations with k-means,” in *Neural Networks: Tricks of the Trade - Second Edition*, pp. 561–580. 2012.
- [23] Leon A. Gatys, Alexander S. Ecker, and Matthias Bethge, “Image style transfer using convolutional neural networks,” in *IEEE Conference on Computer Vision and Pattern Recognition, CVPR*, 2016, pp. 2414–2423.

6. ADDITIONAL RESULTS

6.1. NSN Architecture for Image Generation

Table 3 and Table 4 respectively presents the NSN architectures used for (28×28) MNIST [18] and Fashion [19] and (64×64) LFW [20] and Church [21] datasets. At each layer, we apply stride $\text{step}= 2$ to downsample the feature maps to (approximately) half of its size. Note that, our non-parametric EM algorithm automatically determines the required number of filters during training at each layer of the network.

Layers	Input	Filter, Stride	No. of filters automatically determined during training	
			MNIST	MNIST: Fashion
L0	28×28	$(4 \times 4), 2$	96	140
L1	13×13	$(3 \times 3), 2$	130	238
L2	6×6	$(6 \times 6), 2$	131	256

Table 3: Description of 3-layered NSN architecture applied for (28×28) images of MNIST and Fashion datasets.

Layers	Input	Filter, Stride	No. of filters automatically determined during training	
			LFW	LSUN: Church
L0	64×64	$(4 \times 4), 2$	284	273
L1	31×31	$(3 \times 3), 2$	242	263
L2	15×15	$(3 \times 3), 2$	240	325
L3	7×7	$(3 \times 3), 2$	235	398
L4	3×3	$(3 \times 3), 1$	161	210

Table 4: Description of 5-layered NSN architecture applied for (64×64) images of LFW and Church datasets.

6.2. Sampling from Intermediate layers

NSN-Gen can be applied at any hidden layer to visualize samples at different hidden layers of the network. This can be useful to fine tune the network parameters as well as the convergence of the training algorithms. To generate image patches from layer k , we sample a $1 \times 1 \times N_k$ dimensional noise vector from $\mathcal{N}(\mathbf{0}, \mathbf{1})$; where N_k represents the number of filters at layer k . This noise vector is represented as a patch for the feature map F_k of layer k . Now, we start from layer k and apply NSN-Gen to generate an image patch in the input layer. Figure 8 shows the generated samples from different intermediate layers of NSN, trained on Church dataset [21].

6.3. Manipulating Noise Vectors for Image Generation

Similar to GANs, we can also manipulate the noise vectors z , to manipulate generated images from NSN, revealing rich linear structure of visual concepts established in the noise space

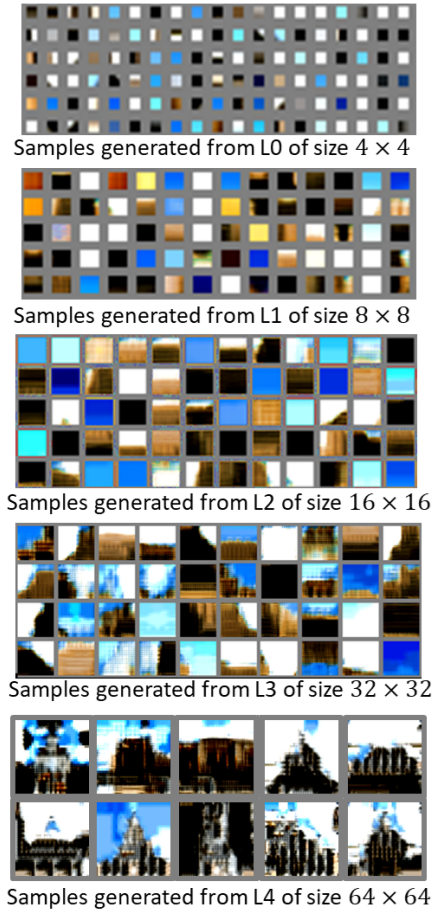


Fig. 8: Visualization of samples generated from the hidden layers of NSN trained on the Church [21] images.

[8]. Further, we can construct a noise vector to generate image from a particular final layer filter of NSN. To generate an image from a filter g_j , we encode the noise as a one-hot vector with all except the j^{th} index as zero and apply NSN-Gen. Note that, images generated from different filters have different visual characteristics. As we can see in Figure 9a, by interpolating the noise vectors corresponding to two different filters, we can generate new images with interpolated visual properties of them. Note that, when NSN is trained with ZCA pre-processed images, due to the inherited sampling properties of NSN-Gen, we obtain different images with similar visual properties as we repeatedly generate samples from the same noise vector.

Further, we can apply simple arithmetic on the final layer NSN filters to generate new images of combined properties (Figure 9b). After choosing the noise vectors corresponding to the filters, we apply NSN-Gen to generate the final-layer input feature maps (i.e F_{L-1}) corresponding from the noise vectors. Now, we apply our desired arithmetic operation on these feature maps and reconstruct the images from the new feature maps.



Images created from Filter-A of last layer of NSN



Images obtained by interpolating Filter-A and Filter-B



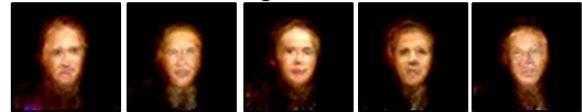
Images created from Filter-B of last layer of NSN

(a) Interpolation between two noise vectors corresponding to two different filters.

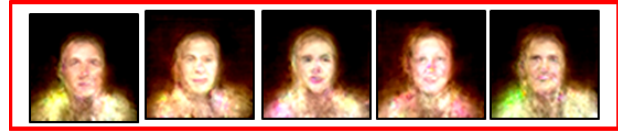
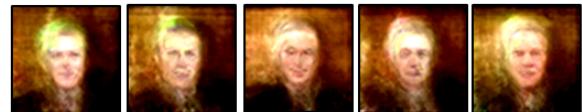
Filter 1: Yellow Background and Colorful cloths



Filter 2: Black Background and Dark Cloths



Filter 3: Yellow Background and Dark Cloths



(Filter1+Filter2-Filter3)

Yellow Background and Dark Cloths

(b) Arithmetic operation among the final layer NSN filters.

Fig. 9: (a) Top and bottom rows are showing the images generated from two different filters. While Filter-A (top row) is generating darker faces in a yellowish background, Filter-B (bottom row) is generating brighter faces in black background. As we can see in the red box, how the attributes of the images are changing as we move from Filter-A to Filter-B by interpolating the noise vector.

(b) Top three rows are showing the generated images from three different filters. To add the features of two filters and subtract it from the third filter, we generate the final-layer input feature map (i.e F_3) and apply the desired arithmetic operation. The resultant feature map is then used to generate the image using NSN-Gen. As we can see, the images generated in the last row are keeping the features of Filter 1 and Filter 2 while throwing away the features of Filter 3.



(a) DCGAN Samples



(b) WGAN Samples



(c) LSGAN Samples

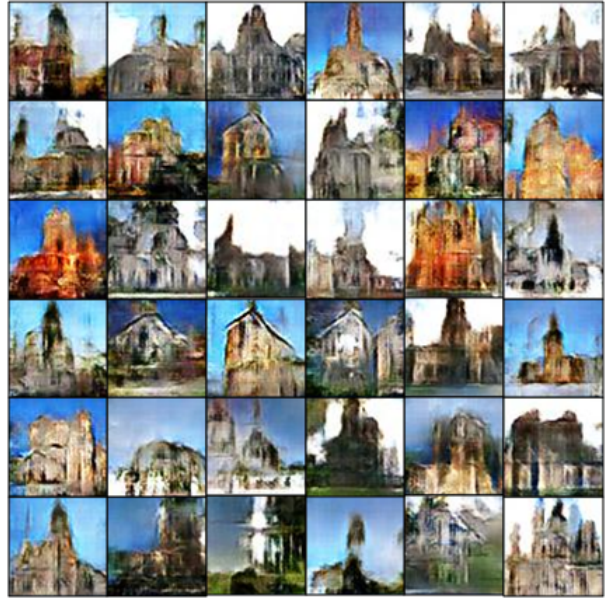


(d) NSN(ours) Samples

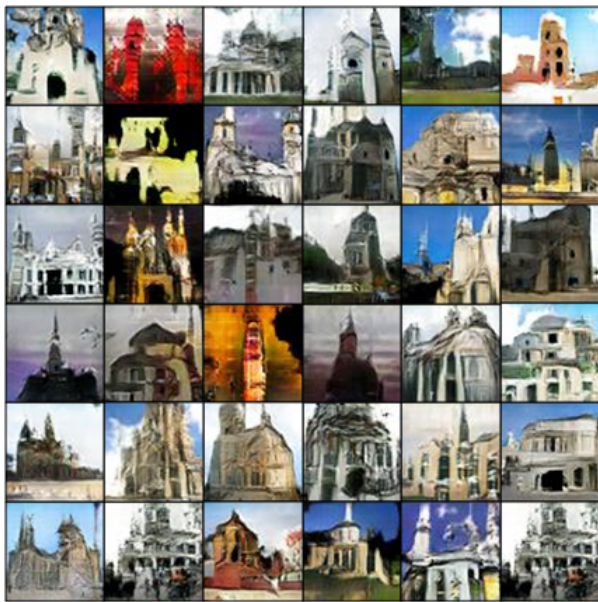
Fig. 10: More examples of generated samples by different state-of-the-art GAN models and our proposed NSN trained on LFW dataset [20].



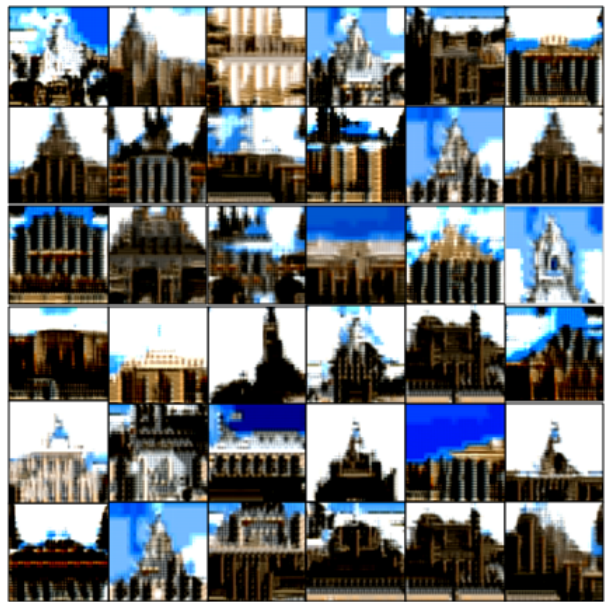
(a) DCGAN Samples



(b) WGAN Samples



(c) LSGAN Samples



(d) NSN(ours) Samples

Fig. 11: More examples of generated samples by different state-of-the-art GAN models and our proposed NSN trained on Church dataset [21].

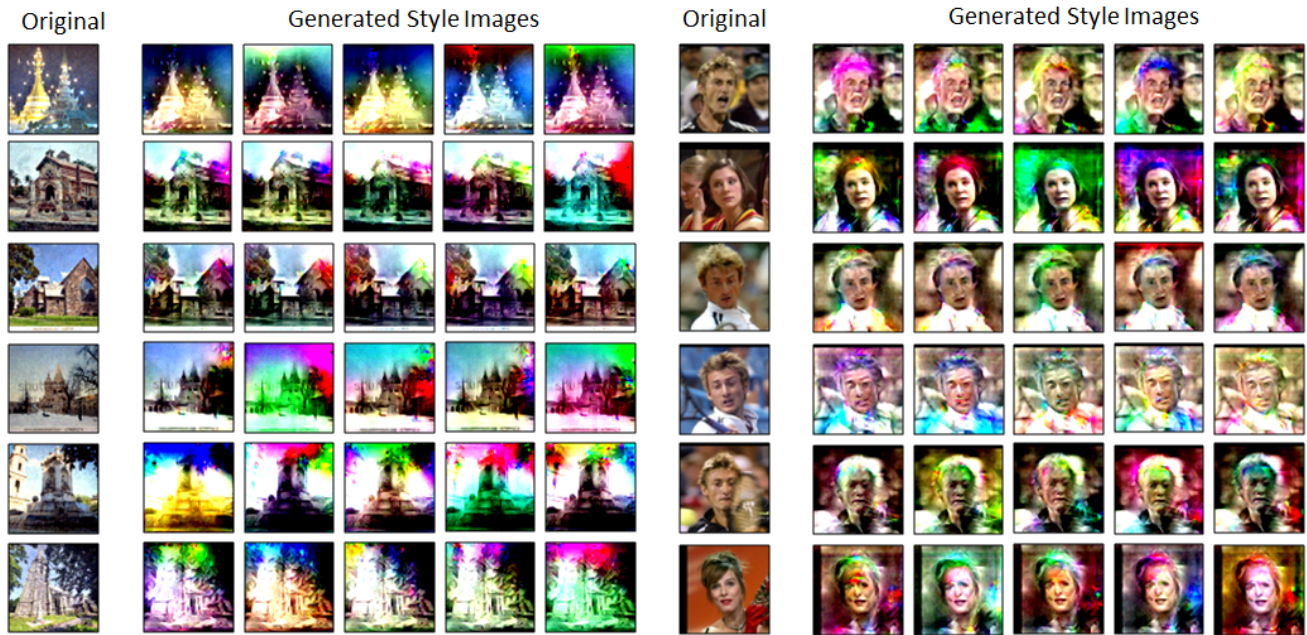


Fig. 12: More examples of generated style images from the proposed NSN. Left: Church [21], Right: LFW [20].



Fig. 13: More example of image reconstruction from occluded images by NSN.